Institute of Physics Publishing Journal of Physics: Conference Series **14** (2005) 228–235
doi:10.1088/1742-6596/14/1/027 Fourteenth International Couette Taylor Workshop

Bicritical instabilities in pressure driven helicoidal flows

A Meseguer and F Marques

Departament de Física Aplicada, Univ. Politècnica de Catalunya,
C/ Jordi Girona 1-3, Mod. B5, 08034 Barcelona, SPAIN

E-mail: alvar@fa.upc.edu

Abstract. This contribution presents new phenomena regarding the stability of pressure driven flows within annular pipes. The fluid is advected downstream due to an axial pressure gradient but also subjected to centrifugal mechanisms due to the independent rotation of the coaxial cylinders that contain it. Coexistence of upstream and downstream spiral secondary flows is observed in the co-rotating regime for a medium gap configuration $\eta = 0.5$ and the boundary bicritical curve is provided for a wide range of angular speeds of the cylinders and axial velocities. A particular computation of the linear stability of the basic flow is carried out for a small gap case with $\eta = 0.77$ in order to detect the unstable modes and recover the also termed as *Double Secondary Spiral Flows* observed experimentally in the past by other authors. The provided linear stability results for this case are, within their limitations, qualitatively consistent with the experimental observations.

.

1. Introduction

Pressure driven swirling flows are of common usage in industry for many purposes such as cooling of rotating electrical machinery, purification of industrial waste water or optical fibre fabrication techniques [11, 2]. Beyond the practical applications of these kind of flows, there are many theoretical aspects that are of interest for the fluid dynamicist regarding the stability of the basic regime. The stability analysis of this type of flows has been studied numerically and experimentally by many authors [9, 3, 4, 12, 6]. A first comprehensive linear stability analysis was provided by the present authors [8] for medium gap, where the study covered a wide range of independent angular speeds of the cylinders as well as axial velocities, but the computations were unresolved in the azimuthal coordinate for moderately high angular speeds of the outer cylinder.

Experiments carried out in the past revealed complex dynamics of the resulting secondary flows, consisting of a superposition of two spiral regimes travelling axially in opposite directions [10, 5], also termed as *Double Spiral Secondary Flow*. Therefore, the main purpose of this study is to provide some numerical evidence of the existence of bicritical bifurcating spiral modes in this type of flows, based on a linear stability analysis of the basic solution with a more accurate exploration in the azimuthal variable.

The paper is structured as follows. Section §2 is devoted to the mathematical formulation of the stability problem. A comprehensive exploration of the bicritical regimes is provided in section §3 for wide gap situations with $\eta = 0.5$, focusing on the effects of large variations in

© 2005 IOP Publishing Ltd

the dominant critical azimuthal modes. Finally, in section §4 a linear stability analysis is also carried out for a small gap case for $\eta = 0.77$ in order to recover the experimental evidences of double spiral flows observed by other authors in the past.

2. Formulation of the problem

An incompressible fluid of kinematic viscosity ν and density ϱ is contained between two concentric rotating cylinders whose inner and outer radii and angular velocities are r_i^*, r_o^* and Ω_i, Ω_o respectively. In addition, the fluid is driven by an imposed axial pressure gradient. The independent dimensionless parameters appearing in this problem are: the radius ratio $\eta = r_i^*/r_o^*$, which fixes the geometry of the annulus; the Couette flow Reynolds numbers $Ri = dr_i^*\Omega_i/\nu$ and $Ro = dr_o^*\Omega_o/\nu$ of the rotating cylinders, where $d = r_o^* - r_i^*$ is the cylinders gap, and the axial Reynolds number, $Re = \bar{w}d/\nu$, where $\bar{w}$ is the mean axial flow in the annulus, and measures the imposed axial pressure gradient.

Henceforth, all variables will be rendered dimensionless using d, d^2/ν, and ν^2/d^2 as units for space, time and the reduced pressure ($p = p^*/\varrho$), respectively. The Navier–Stokes equation and the incompressibility condition for this scaling become

$$\partial_t \mathbf{v} + (\mathbf{v}\cdot\nabla)\mathbf{v} = -\nabla p + \Delta\mathbf{v}, \quad \nabla\cdot\mathbf{v} = 0\,. \tag{1}$$

Let $\mathbf{v} = (u, v, w)$ the physical components of the velocity field in cylindrical coordinates (r, θ, z). The boundary conditions for $\mathbf{v}$ are:

$$v(r_{\rm i}) = Ri, \quad v(r_{\rm o}) = Ro \tag{2}$$

where $r_i = r_i^*/d = \eta/(1-\eta)$, $r_o = r_o^*/d = 1/(1-\eta)$. The steady velocity field $\mathbf{v}_B$ (spiral Poiseuille flow), independent on the axial and azimuthal coordinates (θ, z), and satisfying (1) and (2) is

$$\mathbf{v}_B = (u_B, v_B, w_B) = (0,\ Ar + B/r,\ C\ln(r/r_{\rm o}) + D(r^2 - r_{\rm o}^2)), \tag{3}$$

where $A = (Ro - \eta Ri)/(1+\eta)$, $B = \eta(Ri - \eta Ro)/(1-\eta)(1-\eta^2)$, $C = 2(1-\eta^2)Re/(1-\eta^2 + (1+\eta^2)\ln\eta)$, $D = (1-\eta)(\ln\eta)C/(1+\eta)$. We are going to use through the paper (Ri, Ro, Re) as nondimensional parameters, keeping $\eta = 0.5$ fixed.

The basic flow is perturbed by a small disturbance which is assumed to be periodic in the azimuthal and axial coordinates:

$$\mathbf{v}(r,\theta,z,t) = \mathbf{v}_B + \mathbf{u}(r)\mathrm{e}^{\mathrm{i}(n\theta+kz)+\lambda t}, \tag{4}$$

$$p(r,\theta,z,t) = p_B + q(r)\mathrm{e}^{\mathrm{i}(n\theta+kz)+\lambda t}, \tag{5}$$

where $\mathbf{v}_B = (0, v_B, w_B)$ is given by (3), the azimuthal wave number must be integer ($n \in \mathbb{Z}$), $k \in \mathbb{R}$ and $\lambda \in \mathbb{C}$. The perturbation of the velocity field must be solenoidal and satisfy homogeneous boundary conditions:

$$\mathbf{u}(r_{\rm i}) = \mathbf{u}(r_{\rm o}) = \mathbf{0}. \tag{6}$$

Formal substitution of the perturbed fields (4) and (5) in the Navier–Stokes equations (1) leads to the eigenvalue problem

$$\lambda\mathbf{u} = -\nabla q + \Delta\mathbf{u} - (\mathbf{v}_B\cdot\nabla)\mathbf{u} - (\mathbf{u}\cdot\nabla)\mathbf{v}_B, \tag{7}$$

where nonlinear terms have been neglected. The boundary value problem (7)-(6) is numerically discretized making use of a solenoidal Petrov-Galerkin[1] spectral method already formulated

and tested in the study of other spiral flows [7]. The discretization leads to a generalized eigenvalue problem

$$\lambda \mathbb{G}(\eta, n, k) X = \mathbb{H}(Ri, Ro, Re, \eta, n, k) X, \tag{8}$$

where X contains the coefficients of the spectral approximation of the velocity field $\mathbf{u}$. The problem is then reduced to the computation of the spectrum of eigenvalues of Equation (8), and the condition of criticality is obtained when the rightmost eigenvalue of the spectrum of (8) crosses the imaginary axis ($\Re\lambda = 0$). This condition must be imposed for each set of values of the parameters, resulting in an implicit dependence between the parameters of the perturbation $(n, k, \Im\lambda)$ and the set of Reynolds numbers (Ri, Ro, Re).

The symmetries allow us to restrict the exploration to the cases $Re > 0$ and $Ri > 0$. Furthermore, since the Navier–Stokes equations are real, the complex conjugate of a perturbation (4, 5) is also a solution, and we can change simultaneously the sign of n, k and the imaginary part of λ. Therefore, the exploration in the normal mode analysis can be reduced to the case $k \geq 0$ and $n = 0, \pm 1, \pm 2, \ldots$. When axisymmetric modes, $n = 0$, are dominant in the transition, the bifurcated pattern is the Taylor vortex flow, provided that $k \neq 0$. In addition, if the imaginary part of the rightmost eigenvalue, $\omega = \Im\lambda$, is not zero, these Taylor vortices will travel in the axial direction with constant axial speed $c = \omega/k$. When n and k are nonzero, the eigenvector of the linear problem has the form of a spiral pattern. The wavenumbers n and k, together with ω, fix the shape and speed of the spiral. The angle α of the spiral with a z–constant plane is given by $\tan\alpha = -n/(r_o k) = -(1-\eta)n/k$; the speed of the spiral in the axial direction (on a θ–constant line) is $c = -\omega/k$, and the precession frequency in the azimuthal direction is $\omega_{pr} = -\omega/n$.

Let σ be the real part of the rightmost eigenvalue λ of the spectrum of (8). For negative values of σ, the basic flow is stable under infinitesimal perturbations. When σ is zero or slightly positive, the steady flow becomes unstable and bifurcated secondary flows may appear. As commented before, the spectrum depends on the physical parameters and the axial and azimuthal wavenumbers of the perturbation. As a consequence, $\sigma(Ri, Ro, Re, \eta, n, k)$ is a function which implicitly depends on these variables. For fixed values of η, Ro, Re, and a $(n, k)-$azimuthal-axial normal mode given, the inner Reynolds number $Ri^c(n, k)$ such that $\sigma = 0$ is computed. The critical inner Reynolds number is given by $Ri^c = \min_{n,k} Ri^c(n, k)$, and the corresponding values of n, k are the critical azimuthal and axial wavenumbers n^c, k^c which will dictate the geometrical shape of the critical eigenfunction. Furthermore, the imaginary part of the critical eigenvalue, ω^c, gives the angular frequency of the critical eigenfunction. The critical values Ri^c, n^c, k^c and ω^c are implicit functions of the parameters η, Ro and Re.

3. Bicritical regimes of opposite azimuthal sign for $\eta = 0.5$

The exploration has been focused on the co-rotation region, where the coexistence of negative and positive azimuthal wavenumbers has been detected. Figure 1 shows six curves corresponding to the critical inner rotation Reynolds number Ri^c as a function of the axial Reynolds number Re, and for different values of Ro, ranging from $Ro = 0$ to $Ro = 450$. The transition points between different azimuthal wavenumbers have been represented with white circles, and the dominant value of n^c has also been included for clarity for $Ro = 450$. The folded structure of the critical curves appearing in figure 1 was already pointed out in the analysis carried out in [8], although the negative azimuthal modes were overlooked in that analysis due to a lack of spectral resolution in the angular variable. To visualize the change of sign of n^c, the Ri^c curve for $Ro = 120$ has been included in figure 2. In that curve it can be observed a first transition from the axisymmetric mode $n^c = 0$ to $n^c = 1$ at $Re = 30.82$ and to $n^c = 2$ for $Re = 36.96$. These gradual increasing with $\Delta n^c = \pm 1$ is typical in other confined flows such as Taylor-Couette or Rayleigh-Benard problems. Nevertheless, figure 2 reveals an unexpected change of dominance to negative modes for $Re = 42.75$, where $\Delta n^c = -5$, thus $n^c = -3$ becoming the critical azimuthal wavenumber. This change affects not only the geometry of the secondary patterns appearing at transition, but

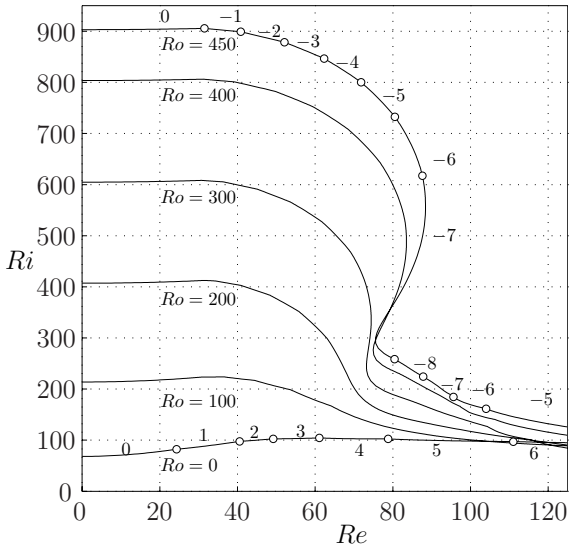

Figure 1. Critical inner rotation Reynolds number Ri^c as a function of Re for the specified values of $Ro \in [0, 450]$. The white circles of the curves $Ro = 0$ and $Ro = 450$ are located at the transition points between different azimuthal wavenumbers n^c, whose values have also been included along the curves.

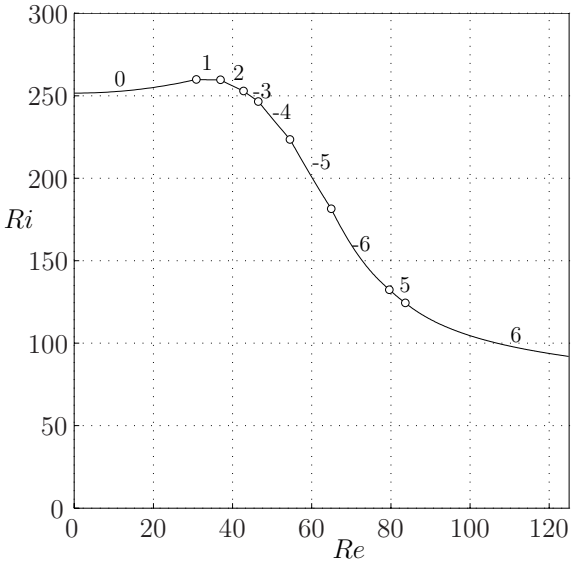

Figure 2. Same as in figure 1 for $Ro = 120$, showing the change of sign of the azimuthal wavenumber from $n^c = 2$ to $n^c = -3$.

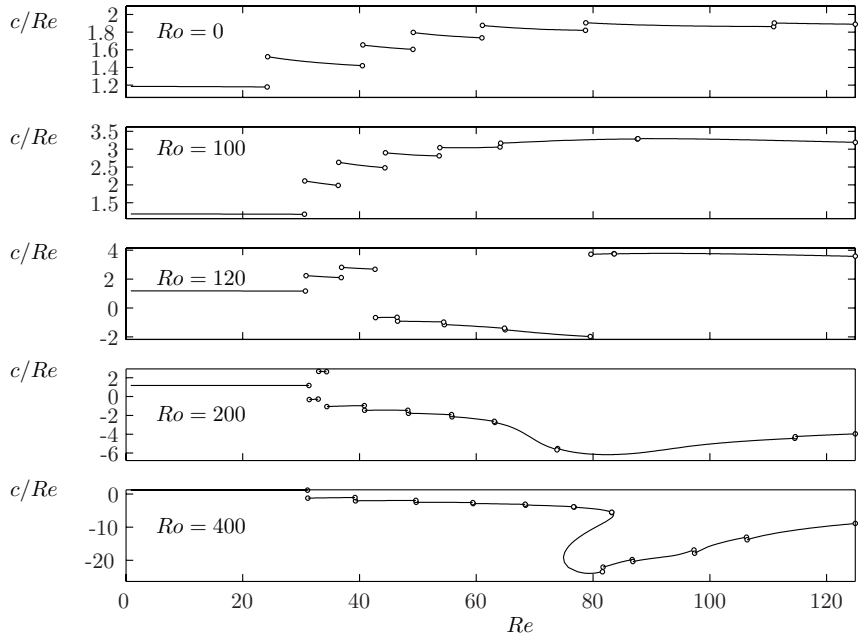

Figure 3. Axial speed of the spirals scaled with the downstream mean flow for $Ro \in [0, 400]$. The white circles correspond to changes in the critical azimuthal wavenumber n^c. Note the large and negative value of c/Re when increasing Ro.

also the propagating speed direction of the resulting travelling waves. This is reflected in figure 3 for some selected values of Ro in figures 1 and 2, where the quantity c/Re has been plotted, representing the axial speed scaled in units of $\bar{w}$, i.e., the relative speed of the spiral with respect to the mean axial flow. For $Ro = 0$ and $Ro = 100$, the spirals propagate downstream with the

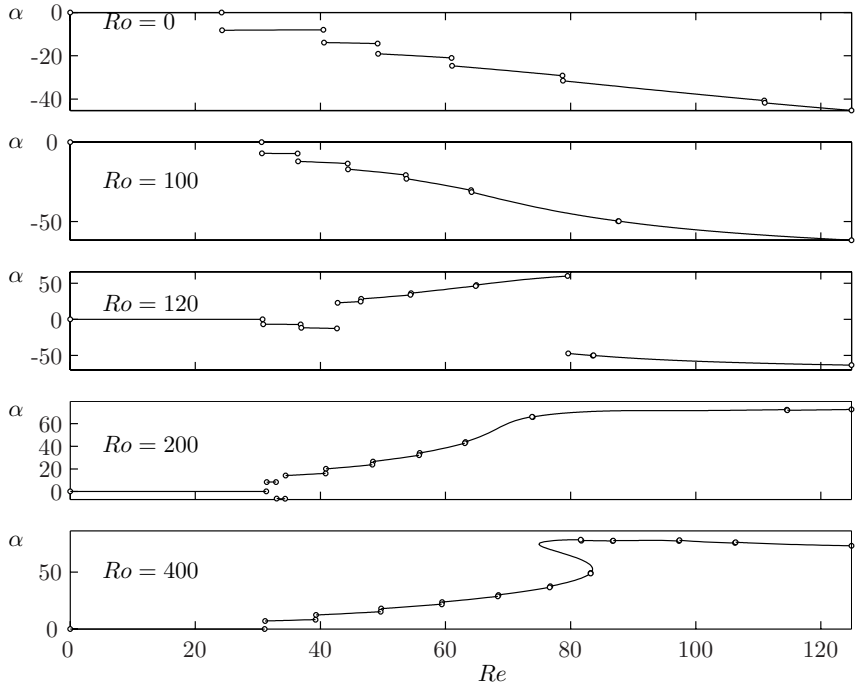

Figure 4. Angle α (in degrees) defined in section §2 corresponding to the secondary patterns for the same parameters as in figure 3. The white circles correspond to changes in the critical azimuthal wavenumber.

mean flow, but slightly faster and with opposite helicoidal orientation to the basic regime. This behaviour changes when increasing Ro and a first evidence is the curve $Ro = 120$, where the axial speed suffers a dramatic change for $Re = 42.75$, associated with the aforementioned change of sign of the azimuthal wavenumber of figure 2. Within the folding region (figure 3, $Ro = 400$), the curves exhibit larger variations of the axial speed of the travelling waves. As an example, for $Ro = 400$ and $Re = 80$, the spirals move upstream nearly thirty times faster than the mean flow and with the same helicoidal orientation, dictated by the angle of the eigenfunction defined in section §2. In figure 4, the angle α of the bifurcating patterns has been plotted for the same values as in figure 3. We focus our attention in the curve $Ro = 120$ of figure 4, where there exists an interval of disconnected bifurcating modes of positive angle bounded by coexisting negative ones. The coexistence of simultaneous bifurcating modes associated with opposite azimuthal sign may result in flows consisting of a superposition of two travelling waves in opposite axial orientations. From a theoretical point of view, it is interesting to study the region in the (Re, Ro)-plane where one ore more azimuthal modes coexist at criticality. The present exploration has provided the curve of bicritical regimes between axisymmetric or positive and negative azimuthal modes. This boundary has been plotted in figure 5, where the gray region corresponds to $n = 0$ (axisymmetric modes), and the regions below and above the curve corresponds to positive and negative azimuthal modes, respectively. The boundary is continuous but not differentiable, due to the fact that the azimuthal wavenumbers are integers. When the outer cylinder is at rest ($Ro = 0$), axisymmetric perturbations are dominant for $Re \lesssim 24.2$. As long as Ro is increased, the threshold value for dominance of axisymmetric disturbances stagnates nearly $Re \sim 31.5$. Nevertheless, the transition from axisymmetric to non-axisymmetric azimuthal modes depends on the value of Ro. For instance, if $Ro < Ro^+ = 189$, the transition is from $n^c = 0$ to $n^c > 0$, whereas above that threshold value the transition leads to negative critical modes. The threshold outer Reynolds number Ro^+ is a function of Re and decreases to a minimum value at the point $(Re, Ro) = (54.11, 106.5)$ and it seems to attain an almost constant value when further increasing the axial Reynolds number. The computation of the asymptotic value of $Ro^+(Re)$ is currently out of the scope of this study.

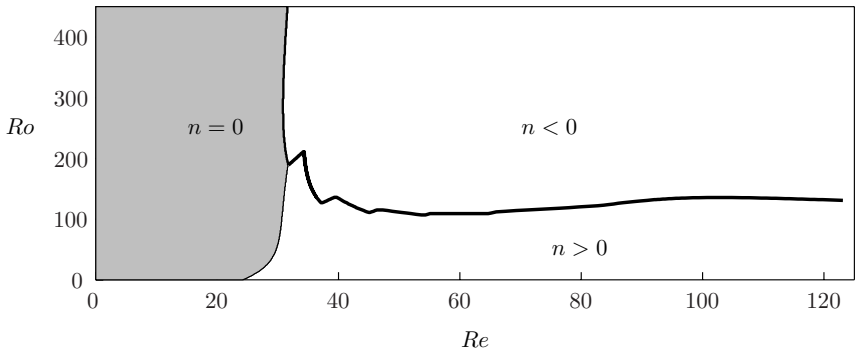

Figure 5. Bicritical boundaries between axisymmetric or positive and negative azimuthal modes for $\eta = 0.5$.

4. Experimental evidence for $\eta = 0.77$

The coexistence of the two spiral regimes has been already reported in the experiments carried out by Nagib in 1972. In his work, Nagib termed this regime as the *Double Spiral Secondary Flow* (DSSF). The comparisons of the present numerical results with the experiments are particularly difficult due to two main reasons. First, the reported experiments where the DSSF was observed were done for a much smaller radius ratio of $\eta = 0.77$, thus activating higher azimuthal modes that are out of the range of the current $\eta = 0.5$ exploration. Second, the numerical results presented here come from a pure linear stability analysis, and not from nonlinear computations. Therefore, our results are only valid in a neighbourhood of the critical regime. Nevertheless, we can overcome the first problem by studying the linear stability analysis for the specified experimental values provided by Nagib.

A particular stability analysis has been carried out for $\eta = 0.77$, with $n \in [-20, 20]$ in order to detect the primary instability for the same values as the ones fixed by the experiments: $Ro = 898$ and $Re = 120$, corresponding to the nondimensional values used by Nagib, $(\mathrm{N}_{\mathrm{R}\theta})_o = 1795$ and $\mathrm{N}_{\mathrm{RZ}} = 240$, respectively. Figure 6 plots the neutral stability curves corresponding to the most dangerous positive and negative azimuthal modes. The dominant positive and negative critical modes are $n^c = 15$ and $n^c = -13$, plotted with thicker lines, with minimum values located at $(k^c, Ri^c) = (0.736, 652.29)$ and $(k^c, Ri^c) = (0.729, 607.35)$, respectively, represented with white circles.

Figure 7 shows a photograph of the observed DSSF for the same values of Re and Ro, but for a higher value of the inner Reynolds number $Ri = 835$, or $(\mathrm{N}_{\mathrm{R}\theta})_i = 1670$, according to Nagib's nondimensionalization. Therefore, a wide range of azimuthal modes have been destabilized by the time the secondary regime has already been established, according to linear computations. An interesting common feature of the two modes $n^c = -13$ and $n^c = 15$ is their almost equal axial periodicity, ranging from $k_c = 0.729$ to $k_c = 0.736$, with less than a 1% deviation, that makes the coexistence of the two regimes possible in a real experiment with finite cylinders, where both critical values of k must be (small) multipliers of $2\pi/L$ (being L the length of the pipes) and their quotient is then rational. In this sense, the case $1:1$ has been found to be optimal.

Figure 8 shows the two stream functions associated with the rightmost bifurcating eigenvalues corresponding to the modes $n = -13$ and $n = 15$, evaluated at their respective linear critical values. Some differences must be pointed out when comparing figures 7 and 8. First, the computations plotted in figure 8 correspond to the eigenvectors associated to the rightmost eigenvalues for the previously computed critical values $Ri^c_{-13} = 607.35$ and $Ri^c_{15} = 652.29$, and not for $Ri_{\mathrm{exp}} = 835$, as shown in figure 7. Second, the represented flow in figure 8 *does not* include the basic flow, whereas in figure 7 the observed flow must necessarily contain an axial and azimuthal component not present in our computations. Nevertheless, there is a very good agreement between both patterns. More information, such as the propagating axial speeds of

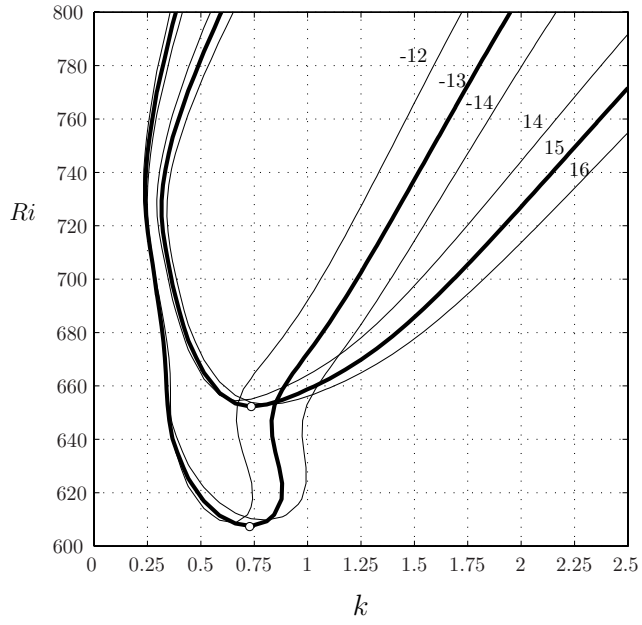

Figure 6. Neutral stability curves $\sigma(k, Ri) = 0$ corresponding to the azimuthal modes for $\eta = 0.77$, $Ro = 898$ and $Re = 120$. The bolded curves correspond to the dominant modes $n = -13$ and $n = 15$. The neighboring modes $n = -14, -12, 15$ and 16 have been included for clarity.

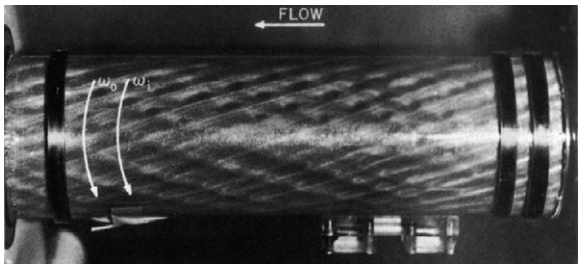

Figure 7. Experimental DSSF observed by Nagib for $\eta = 0.77$.

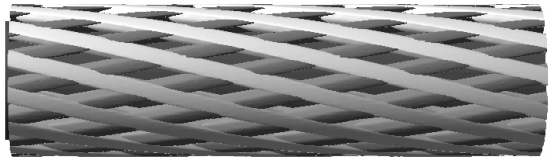

Figure 8. Computed streamfunctions associated to the azimuthal modes $n = -13$ and $n = 15$ at their critical values for $\eta = 0.77$.

the patterns, would be required to confirm the identity of the modes shown in figure 7. Nagib carried out a comprehensive study of the geometrical features of the secondary flows appearing in this problem but, unfortunately, the axial speeds of the DSSF spirals are not reported in his work. Of course, the neighboring modes $n = -12, -14$ and $n = 14, 16$ may be at work as well and nonlinear direct numerical simulations would be necessary to clarify their role. We have considered the modes $n = -13$ and $n = 15$ as the most representative and plausible ones because of their almost coincident axial periodicity and linear dominance within the studied range of parameters.

5. Conclusions

Pressure driven helicoidal flows through annuli may exhibit secondary flows consisting of double spiral flows that are characterized by the coexistence of spiral waves travelling in opposite directions. A linear stability analysis reveals that this phenomenon might be observed for wide gap cases in the co-rotating regime and for a continuous set of points that prescribes a boundary in the parameter space. Experimental observations carried out for small gap configurations confirm the existence of this kind of patterns and a linear stability analysis carried out for the same values of the experimental parameters predicts the existence of these coexisting solutions, but for much higher azimuthal modes, compared with the wide gap case. The agreement between

linear computations and experiments is, within its limitations, excellent, although nonlinear computations should be carried out in order to clarify the nature of the secondary solutions and their stability. Nonlinear studies are currently in progress.

Acknowledgments
This work was supported by the Spanish Ministry of Science and Technology, grant FIS2004-01336.

References

[1] Canuto C, Hussaini M Y, Quarteroni A and Zang T A 1988 *Spectral Methods in Fluid Dynamics* (Berlin: Springer-Verlag)
[2] Chida K, Sakaguchi S, Wagatsuma M and Kimura T 1982 *Electronic Letters*, **18** 713
[3] Chung K C and Astill K N 1977 *J. Fluid Mech.* **81** 641
[4] Hasoon M A and Martin B W 1977 *Proc. Roy. Soc. A* **352** 351
[5] Joseph D D 1976 *Stability of Fluid Motions I and II, Springer Tracts in Natural Philosophy* (Berlin: Springer-Verlag)
[6] Lueptow R M, Docter A and Min K 1992 *Phys. Fluids A* **4** 2446
[7] Meseguer A and Marques F 2000 *J. Fluid Mech.* **402** 33
[8] Meseguer A and Marques F 2002 *J. Fluid Mech.* **455** 129
[9] Mott J E and Joseph D D 1968 *Phys. Fluids* **11** 2065
[10] Nagib H M 1972 *On instabilities and secondary motions in swirling flows through annuli* Ph. D. dissertation, Illinois Institute of Technology
[11] Ollis D F, Pelizzetti E and Serpone N 1991 *Environ.Sci.Technol.* **25** 1523
[12] Takeuchi D I and Jankowski D F 1981 *J. Fluid Mech.* **102** 101